

Supplement of Biogeosciences, 18, 961–975, 2021
<https://doi.org/10.5194/bg-18-961-2021-supplement>
© Author(s) 2021. This work is distributed under
the Creative Commons Attribution 4.0 License.



Supplement of

Methane efflux from an American bison herd

Paul C. Stoy et al.

Correspondence to: Paul C. Stoy (pcstoy@wisc.edu)

The copyright of individual parts of the supplement might differ from the CC BY 4.0 License.

Supplemental Information

Bison demographics and feed

The land managers provided information that describes bison age, sex, weight, and pregnancy status (Table S1) and the composition (Table S2) and the delivery schedule (Table S3) of hay.

Tikhonov Regularization

To briefly describe the motivation for using Tikhonov Regularization for our case, consider the extreme distributions of potential bison locations: all are located in a single grid cell (a Dirac delta function) or all are perfectly distributed across the field (an uninformed prior). The true distribution likely exists between these cases, especially given intermittent bison movements. All observations have uncertainty so estimates of bison location using cameras provides an initial guess of the true location. We assume that the true number of each bison in each pixel is likely to be similar to those measured in adjacent pixels because the bison movements were usually minor and because of the uncertainty that exists when attempting to associate bison to a particular pixel. Two-dimensional Tikhonov Regularization can estimate the likelihood of the location elements (here bison) given the constraints that the distribution is bounded and that adjacent pixels are likely similar to a given pixel (Stoy and Quaife, 2015).

We use a form of Tikhonov Regularization to create spatial disaggregation of each bison distribution map (α') following Stoy and Quaife (2015):

$$\alpha' = \alpha(I + \gamma^2 B^T B)^{-1} \frac{\sigma^2}{\psi(\gamma^2)} - \mu_\alpha + \mu_{\alpha'}. \quad (S1)$$

Here, α is the measured distribution map with mean μ_α (the number of bison per pixel) and variance σ , I is the identity matrix, B represents the constraint that neighboring elements should be similar by requiring a first difference of zero in the cardinal directions of the map, γ is the Lagrange Multiplier, and $\psi(\gamma^2)$ is a normalization term equal to the variance of $\alpha(I + \gamma^2 B^T B)^{-1}$. Large values γ constrain each pixel to be near the overall mean such that the bison likelihood map is smoother across space.

To explore the sensitivity of flux estimates using Tikhonov Regularization alone, we applied it approach to each bison distribution map using Lagrange multipliers that ranged from 0.1 to 4 and rounded values to the nearest integer to create maps that were highly distributed, as demonstrated for a single half-hour period in Figure S2. Note that the simulation with a Lagrange multiplier of 4 results in a simulation where bison are widely distributed across segments of the field and amounts to a highly conservative estimate of their location. Per-animal flux estimates are also sensitive to the estimates of their location within the field; mean methane flux estimates ranged from 43 – 58 $\mu\text{mol bison}^{-1} \text{ s}^{-1}$ when applying the Hsieh et al. (2000) model and 50 – 75 $\mu\text{mol bison}^{-1} \text{ s}^{-1}$ when applying the Kljun et al. (2015) model after spatial smoothing using Tikhonov Regularization (Figure S3). In other words, Per-bison flux estimates generated using this approach varied by <25% from the value without Regularization on average (Figure S3), implying that even a poor knowledge of bison location (e.g. Fig. S2D) changed per-animal flux estimates by that amount.

Supplemental Tables

Table S1: The sex, age, and pregnancy status of the study bison with weight measured on November 16, 2017 shortly before they entered the pasture on November 17, 2017. Bison were assumed to be born on June 1 of the birth year by the landowners such that animals born in 2017 were nearly 6 months old when measurements began.

Sex	Age (years)	Weight (kg)	Pregnant
F	7.5	467	Y
F	7.5	419	Y
F	7.5	428	Y
F	7.5	479	Y
F	7.5	510	Y
F	7.5	476	Y
F	7.5	492	Y
F	7.5	454	Y
F	7.5	567	Y
F	7.5	476	Y
F	7.5	497	Y
F	7.5	460	Y
F	7.5	443	Y
F	7.5	435	Y
F	7.5	426	Y
F	7.5	476	Y
F	7.5	411	Y
M	5.5	646	
M	5.5	701	
F	3.5	381	Y
F	3.5	410	Y
F	1.5	334	
F	0.5	110	
F	0.5	144	
M	0.5	160	
F	0.5	166	
M	0.5	138	
M	0.5	152	
M	0.5	147	
M	0.5	183	
F	0.5	96	
M	0.5	208	
M	0.5	104	
M	0.5	163	
F	0.5	127	
M	0.5	136	
M	0.5	165	
M	0.5	126	
F	0.5	127	

Table S2: Composition of the first cut and second cut hay provided as a supplement to the study bison herd.

Variable (% unless otherwise noted)	First cut	Second cut
Crude Protein	9.7	17.2
Acid detergent fiber	47.9	38.3
Total digestible nutrients	48.9	59.7
Calcium	0.8	1.51
Phosphorus	0.2	0.21
Magnesium	0.21	0.32
Potassium	1.92	2.06
Sulfur	0.15	0.32
Sodium	<0.011	0.028
Zinc (mg/kg)	14	15
Iron (mg/kg)	66	61
Manganese (mg/kg)	60	56
Copper (mg/kg)	7	9

Table S3: The number of bails of first cut and second cut hay (Table S2) delivered to the bison pasture. The average mass of the first cut bails is 506 kg and the average mass of the second cut bails is 593 kg.

Date	First cut	Second cut
Nov. 17, 2017	2	2
Nov. 20, 2017		2
Nov. 22, 2017	1	2
Nov. 25, 2017		2
Nov. 27, 2017	2	2
Nov. 29, 2017		2
Dec. 1, 2017		2
Dec. 3, 2017		
Dec. 5, 2017	2	2
Dec. 8, 2017	2	2
Dec. 12, 2017		2
Dec. 15, 2017	2	2
Dec. 19, 2017	2	2
Dec. 21, 2017	2	2
Dec. 26, 2017	2	2
Dec. 28, 2017	2	2
Dec. 31, 2017	2	2
Jan. 2, 2018	2	2
Jan. 5, 2018	2	2
Jan. 8, 2018	2	2
Jan. 11, 2018	2	2
Jan. 15, 2018	2	2
Jan. 18, 2018	2	2
Jan. 22, 2018	2	2
Jan. 26, 2018		2
Jan. 27, 2018	2	
Jan. 29, 2018	1	1
Jan. 31, 2018	1	1
Feb. 3, 2018	2	2

Supplemental Figures

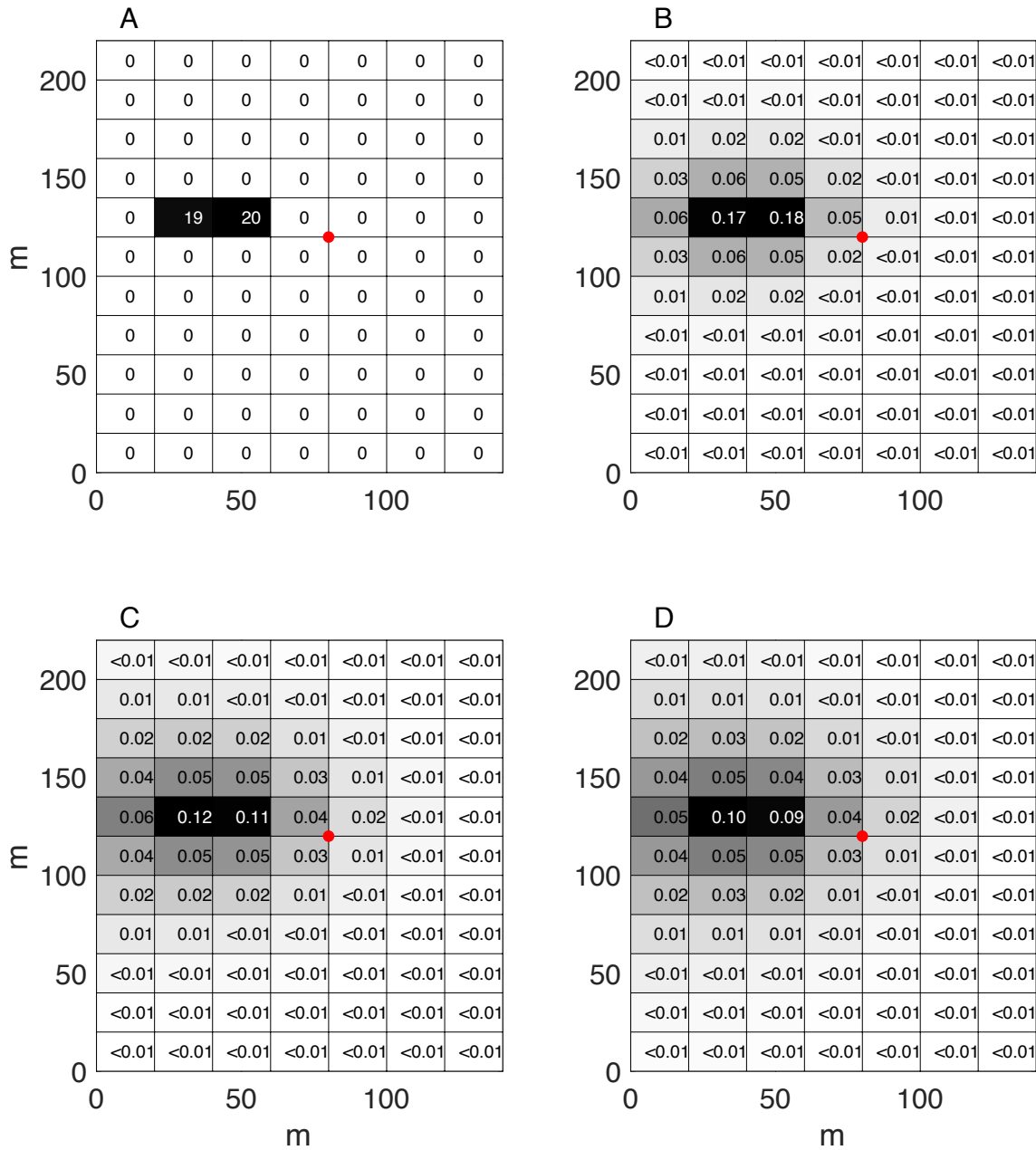


Figure S1: The number of bison observed per grid cell at 9:00 on January 22, 2018 (A) and a the probability of bison landing in each respective grid cell for the stochastic simulations generated using two-dimensional Tikhonov Regularization with Lagrange multipliers of 0.1 (B), 0.3 (C), and 0.5 (D).

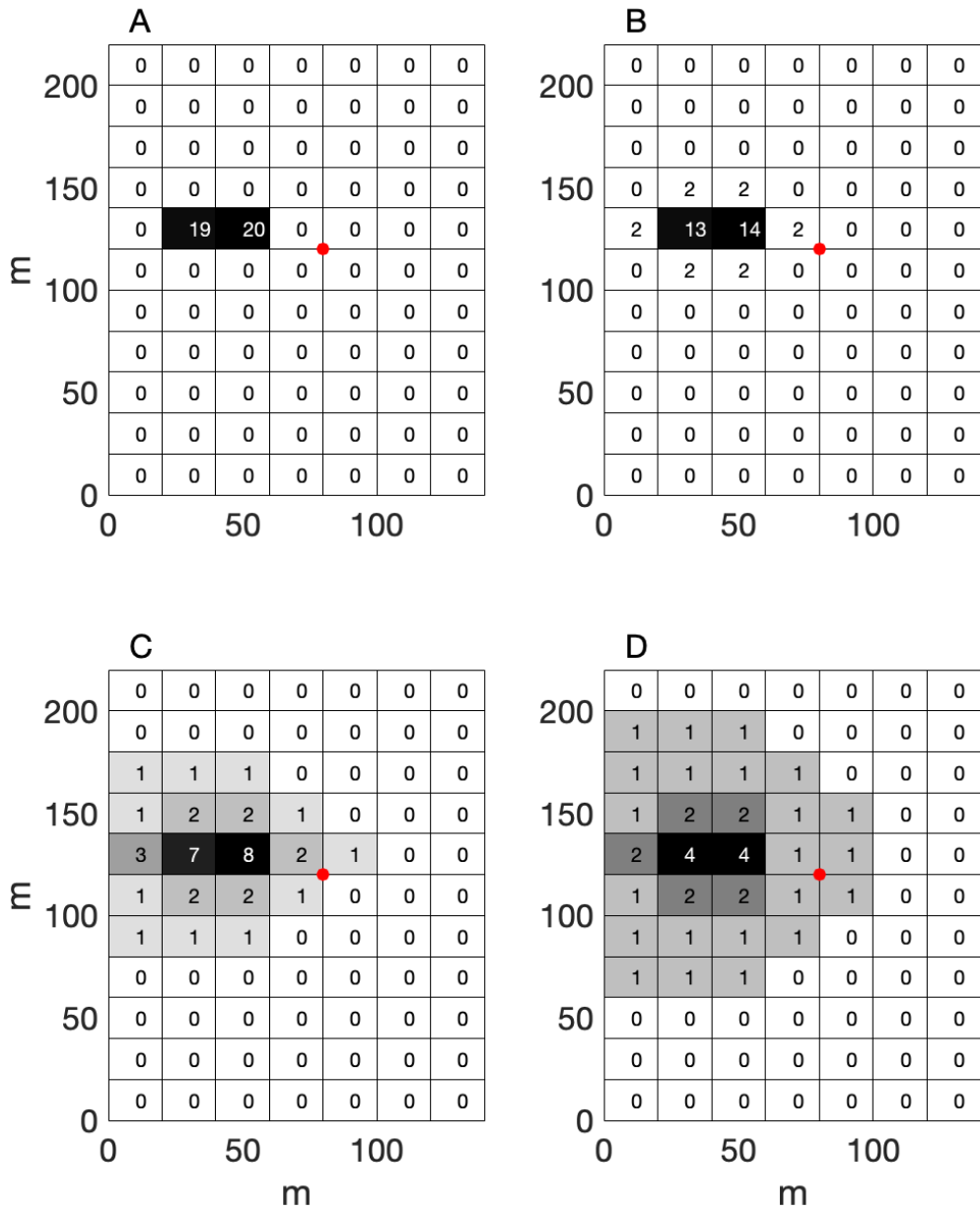


Figure S2: The number of bison observed per grid cell at 9:00 on January 22, 2018 (A) and a distributed bison location map generated using two-dimensional Tikhonov Regularization without stochastic simulation and with Lagrange multipliers of 0.1 (B), 1 (C), and 4 (D).

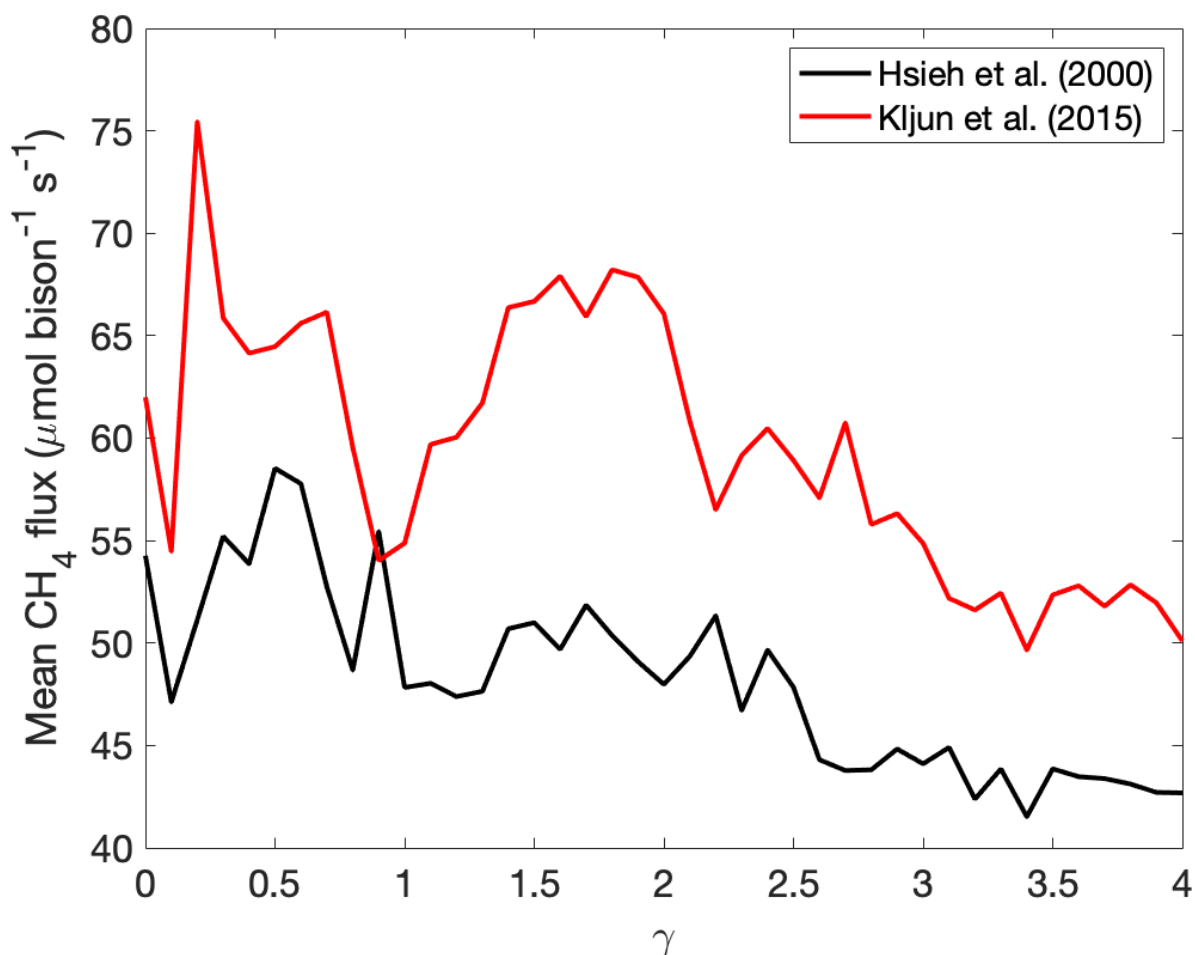


Figure S3: Mean methane efflux on a per-bison basis as a function of spatial smoothing of bison location estimates using the two-dimensional Tikhonov Regularization approach described in Stoy and Quaife (2015) for different values of the Lagrange multiplier γ and the footprint models of Hsieh et al. (2000) and Kljun et al. (2015).